Bacteriochlorins with a Twist: Discovery of a Unique Mechanism to Red-Shift the Optical Spectra of Bacteriochlorins

Matthew J. Guberman-Pfeffer,[†] Jordan A. Greco,[†] Lalith P. Samankumara,[†] Matthias Zeller,[‡,∥] Robert R. Birge,*[,†,§] José A. Gascón,*[,†] and Christian Brückner*[,†]

[†]Department of Chemistry, University of Connecticut, Storrs, Connecticut 06269-3060, United States
[‡]Department of Chemistry, Youngstown State University, One University Plaza, Youngstown, Ohio 44555-3663, United States
[§]Department of Molecular and Cell Biology, University of Connecticut, Storrs, Connecticut 06269-3125, United States

S *Supporting Information*

ABSTRACT: Owing to their intense near infrared absorption and emission properties, to the ability to photogenerate singlet oxygen, or to act as photoacoustic imaging agents within the optical window of tissue, bacteriochlorins (2,3,12,13-tetrahydroporphyrins) promise to be of utility in many biomedical and technical applications. The ability to fine-tune the electronic properties of synthetic bacteriochlorins is important for these purposes. In this vein, we report the synthesis, structure determination, optical properties, and theoretical analysis of the electronic structure of a family of expanded bacteriochlorin analogues. The stepwise expansion of both pyrroline moieties in near-planar *meso*-tetraarylbacteriochlorins to morpholine moieties yields ruffled mono- and bismorpholinobacteriochlorins with broadened and up to 90 nm bathochromically shifted bacteriochlorin-like optical spectra. Intramolecular ring-closure reactions of the morpholine moiety with the flanking *meso*-aryl groups leads to a sharpened, blue-shifted wavelength λ_{max} band, bucking the general red-shifting trend expected for such linkages. A conformational origin of the optical modulations was previously proposed, but discrepancies between the solid state conformations and the corresponding solution state optical spectra defy simple structure-optical property correlations. Using density functional theory and excited state methods, we derive the molecular origins of the spectral modulations. About half of the modulation is due to ruffling of the bacteriochlorin chromophore. Surprisingly, the other half originates in the localized twisting of the $C_\beta-C_\alpha-C_\alpha-C_\beta$ dihedral angle within the morpholine moieties. Our calculations suggest a predictable and large spectral shift (2.0 nm/deg twist) for morpholine deformations within these fairly flexible moieties. This morpholine moiety deformation can take place largely independently from the overall macrocycle conformation. The morpholinobacteriochlorins are thus excellent models for localized bacteriochlorin chromophore deformations that are suggested to also be responsible for the optical modulation of naturally occurring bacteriochlorophylls. We propose the use of morpholinobacteriochlorins as mechanochromic dyes in engineering and materials science applications.
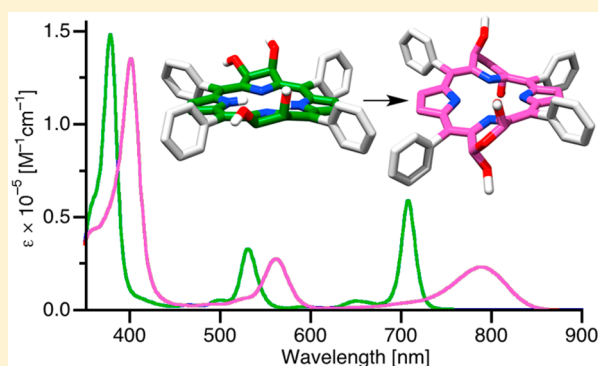
INTRODUCTION

Hydroporphyrins are the key light harvesting pigments in nature.[1] While algae and higher plants utilize chlorophylls, the green Mg(II) complexes of 2,3-dihydroporphyrins (chlorins), the photosynthetic pigments of the anoxygenic phototropic purple bacteria, are Mg(II) complexes of 2,3,12,13-tetrahydroporphyrins (bacteriochlorins), such as bacteriochlorophyll *a*, **1**.[2] The solid state conformations of the naturally occurring bacteriochlorins are overall planar with only minor deviations from the mean plane in each of the pyrroline rings.[3] However, local distortions in select examples were suggested as being important for spectral tuning.[4]

While the conformational modulation of the electronic properties of natural and synthetic porphyrins through steric crowding of their periphery or through protein interactions is

Bacteriochlorophyll *a*, **1**
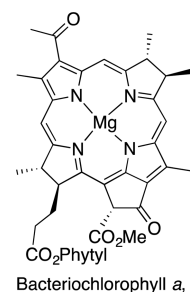
well-known,[5] the corresponding modulation of the more flexible hydroporphyrins in general,[6] and bacteriochlorins in

particular,[4,7] was much less studied. Moreover, the conformational effects in hydroporphyrin analogues containing six-membered rings may be subject to unique effects,[8] but have not been the focus of any systematic study,[9] even though computations of the electronic properties of hydroporphyrin optical spectra are well-described.[6c,10]

Bacteriochlorins possess characteristic three-band absorption spectra, including a high-intensity Soret feature (B band) and two spectrally distinct Q bands, Q_x and Q_y, whereby the longest absortion band Q_y band (also referred to as the λ_{max} band) lies well above 700 nm.[11] Because bacteriochlorins absorb strongly within the spectroscopic window of tissue (the range between ~700 and well above 1000 nm; light of 735 nm possesses the deepest penetration depth in tissue),[12] significant efforts have been devoted to the synthesis and spectral modulation of bacteriochlorins for their utilization as photochemotherapeutics,[13] imaging agents,[14] or optical labels.[13e,15] The NIR absorption properties can also be beneficial for their utility as chemosensors[16] or light-harvesters.[17] An understanding of the conformational modulation of the electronic properties of bacteriochlorins is therefore of broad interest.

Synthetic bacteriochlorins can be prepared by total syntheses,[18] by semisynthetic approaches using naturally occurring tetrapyrroles,[13b,15a,19] and by conversion of synthetic porphyrins.[14b] The latter option remains attractive because of its simplicity, but this methodology also presents some limitations.[14b] Among the potential problems, simple reductions of $C_\beta-C_\beta$ double bonds may be reversible under ambient conditions.[20] Irreversible addition reactions to generate chemically more robust bacteriochlorins are frequently subject to regio- and stereochemical complications.[21] We, and others,[22] described the OsO4-mediated dihydroxylation of meso-arylporphyrin 2[Ar] to generate the corresponding 2,3-vic-dihydroxychlorins 3[Ar] and regioselectively[23] the 2,3-vic-12,13-vic-tetrahydroxybacteriochlorins 3[Ar] as a mixture of two separable stereoisomers (Scheme 1).[24]

In an approach that has no precedent in nature, we explored a range of functional group conversions of one or two dihydroxypyrroline moieties into nonpyrrolic heterocycles, thus generating chlorin and bacteriochlorin analogues carrying a number of different functional groups and possessing a range of optical properties; we dubbed our approach the 'breaking and mending of porphyrins'.[8,9b,c] Others developed related hydroporphyrinoid analogues either through porphyrin conversion or total synthesis.[9b] For instance, the isomeric planar porphodilactones 7-I and 7-II, prepared by Zhang and co-workers, proved valuable in understanding the electronic modulation of the chlorophylls.[25] The presence of the oxazolinone (or, when the carbonyl is reduced, oxazoline) moieties also introduced a number of other unexpected advantages over the parent porphyrins or hydroporphyrins with respect to biodistribution, catalytic activity, the ability to photosensitize lanthanides, or the red-shifts of their spectra.[26]
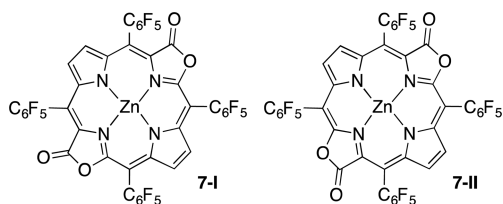
One of the conversions of the dihydroxypyrroline moiety in the chlorin series (3[Ar]) was the ring-expansion to a morpholine

Scheme 1. Syntheses of Chlorin Diols 3[Ar] and Bacteriochlorin Tetraols 4[Ar] by OsO4-Mediated Dihydroxylation of a meso-Tetraarylporphyrin, and Ring-Expansion of Chlorin 3[Ar] to Morpholinochlorin 5[Ar]
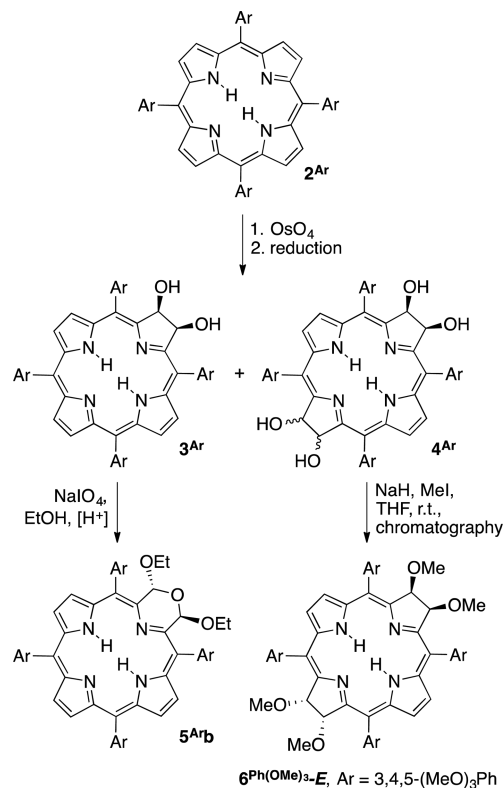

moiety (5[Ar]) (Scheme 1).[27] This conversion resulted in the formation of nonplanar chlorin-type chromophores of persistent chirality with bathochromically shifted optical spectra. In a preliminary report, we also described the conversion of one or two dihydroxypyrrolines in the tetrahydroxybacteriochlorins 4[Ar] into morpholine moieties.[7b] The resulting products were severely nonplanar chromophores possessing all identical bacteriochlorin-type 18 π-electron systems, but with significantly bathochromically shifted and broadened bacteriochlorin-type optical spectra.[28]

While the interpretation that the optical shifts resulted from the nonplanarity of the chromophore was highly suggestive,[7b] a number of observations were seemingly contradictory: The most nonplanar molecule was not the most red-shifted chromophore, and the shifts of the Q_x and Q_y bands showed opposite trends in some cases. Though crystal packing effects could not be excluded to explain some phenomena (all structural data were attained through single crystal diffraction analysis), these observations also highlighted how little is known about the molecular origin of the conformational modulation of bacteriochlorin-type chromophores.

In this contribution, we present the full details to the synthesis, optical properties, and single crystal structure analyses of the mono- and bismorpholinobacteriochlorins. Using density functional theory (DFT) and excited state methods, we delineate the origins of the optical shifts as a combination of two largely independent contributions that arise through ruffling of the bacteriochlorin $C_{16}N_4$ chromophore and, described first here, twisting within the morpholine moiety, while the presence of the ring oxygen(s) or coplanar

Scheme 2. Synthesis of the Morpholinobacteriochlorins by Ring-Expansion of Dihydroxypyrrolines of Bacteriochlorins along the "Breaking and Mending" Strategy
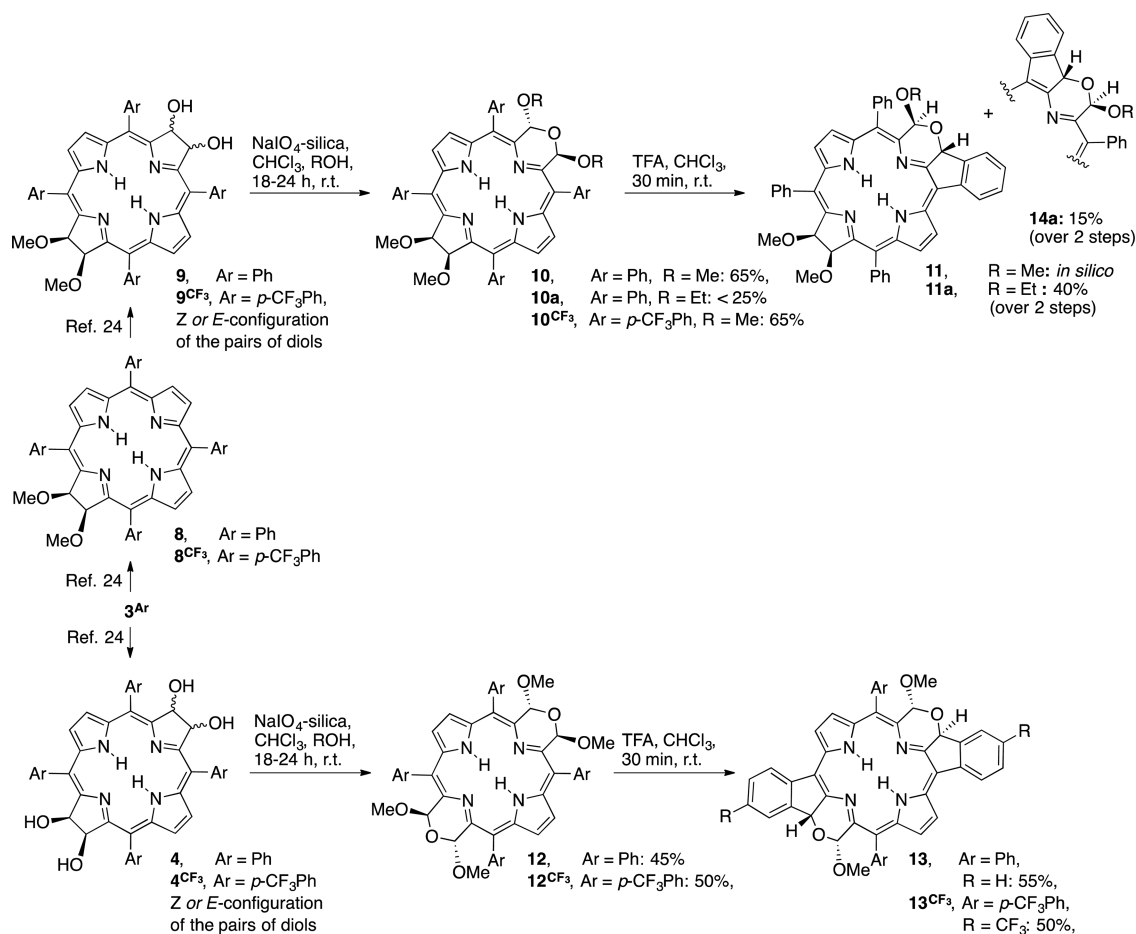

meso-phenyl groups have only minor electronic effects. This study thus delineates some design principles to tune the physicochemical properties of *meso*-arylbacteriochlorins in the NIR region of the electromagnetic spectrum through "single point mutations" of the macrocycle. The conclusions derived may underline the mode of chromophore modulations of certain bacteriochlorins found in nature. The findings also point at a class of dyes for mechanochromic applications.

■ RESULTS AND DISCUSSION

Syntheses and Solid State Structures of Morpholino-bacteriochlorins. Dihydroxylation of known dimethoxychlorins 8^{Ar}, prepared by alkylation of the corresponding dihydroxychlorins 3^{Ar}, generates regiospecifically the dimethoxy-protected tetrahydroxybacteriochlorins 9^{Ar} (Scheme 2).[24] We subjected this bacteriochlorin diol to the mild oxidation conditions ($NaIO_4$, heterogenized on silica gel, $CHCl_3$, alcohol, ambient temperature) known to cleave the diol functionality to generate a secochlorin bisaldehyde and to ring-close this intermediate in situ to form a dialkoxy-substituted morpholine moiety, leading to a single product in satisfying yields.[27b] Based on the diagnostic NMR signals for the morpholino moiety,[27b] it could be characterized as morpholinobacteriochlorin 10^{Ar}, an assignment proven for 10^{CF_3} by X-ray diffractometry.[29] We will discuss the UV–vis spectra of 10^{Ar} and all other bacteriochlorin analogues prepared in detail below; for their fluorescence emission spectra, see the Supporting Information (SI).

The variation of the *meso*-aryl groups (Ph vs *p*-CF3−Ph) had no effect on the principal chemistry observed, the optical properties, or the molecular structure (see the SI), but the crystallinity of the CF3-substituted materials was frequently higher than that of the parent phenyl-substituted analogues, and their ^{1}H NMR spectra were somewhat simplified, facilitating their analysis. In the following, we will discuss the *meso*-aryl derivatives interchangeably. The variation of the morpholine alkoxy groups likewise had no effect on the optical spectra of the derivatives, but some effect on the crystallinity of the products and it induced a profound difference in the chemical stability of the derivatives. The methoxy derivatives were generally more robust than the corresponding ethoxy derivatives.

The parent benchmark bacteriochlorin tetramethoxybacteriochlorin 6^{Ar}, such as $6^{Ph(OMe)_3}$-*E* shown, possesses only a very slightly ruffled chromophore (Figure 1).[24] The conformation is not affected irrespective of the relative stereochemistry of the two pairs of diol groups or whether they are unprotected or methyl-protected.[24] The pyrroline moieties are slightly non-planar because of the strain that is introduced to avoid an unfavorable eclipsed conformation of the two *vic*-methoxy groups, but this distortion translates only minimally into the rest of the macrocycle. In contrast, the introduction of a single oxygen atom into the bacteriochlorin framework has dramatic structural consequences: The conformation of morpholinobacteriochlorin 10^{CF_3} is severely nonplanar.[7b] It is significantly more ruffled than the corresponding morpholinochlorins (such
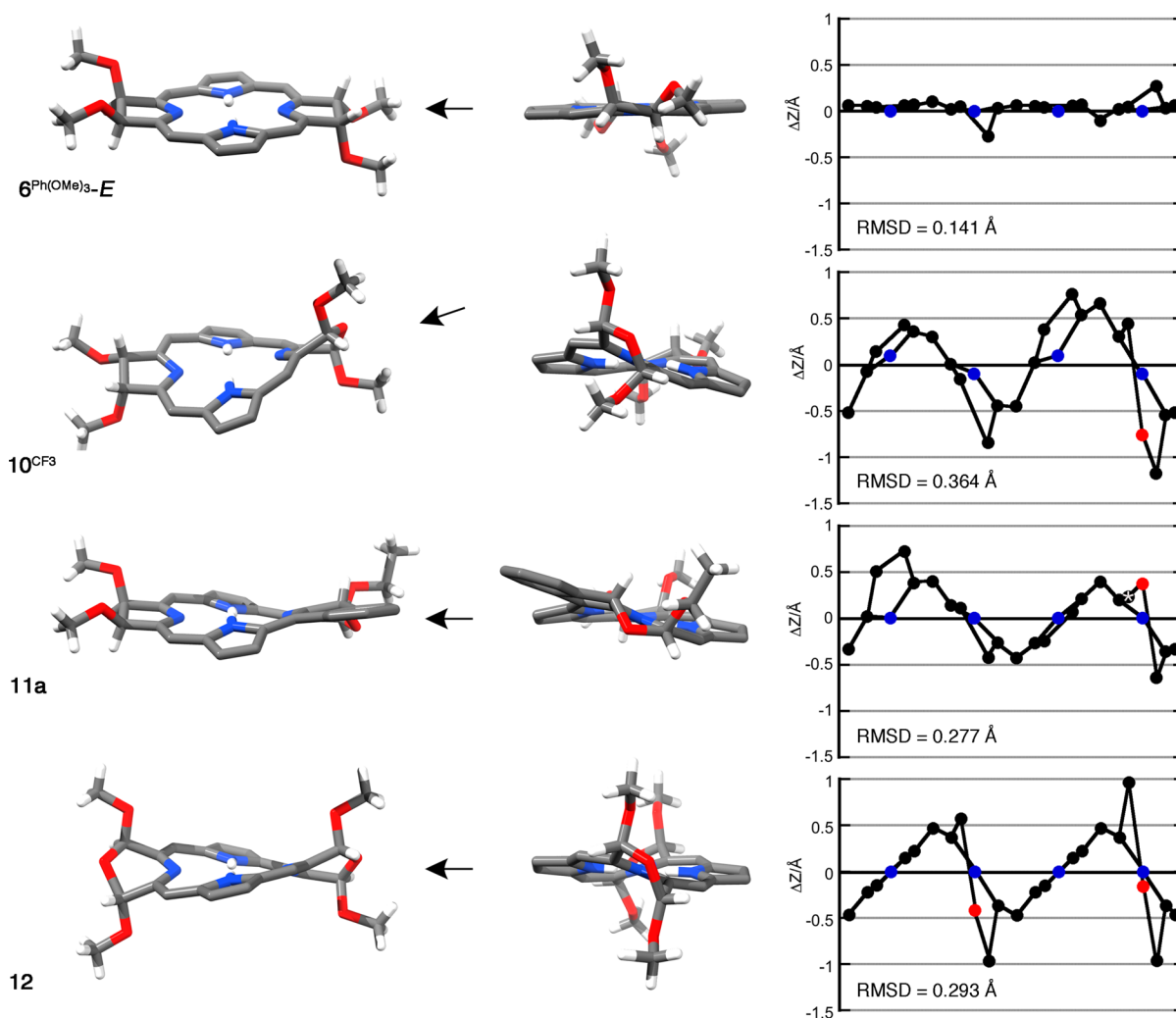
Figure 1. Capped stick models of the molecular structures of bacteriochlorin $6^{Ph(OMe)_3}$-E (CCDC 756651),[32] morpholinobacteriochlorins 10^{CF_3} (CCDC 855681),[7b] monofused morpholinobacteriochlorins **11a** (CCDC 855679),[7b] and bismorpholinobacteriochlorin **12** (CCDC 855680).[7b] Disorder and solvent molecules, all *meso*-aryl groups and sp²-C*H* omitted for clarity. Left column: Oblique views, chosen such that the distant pyrrole moiety is viewed from a similar perspective. Middle column: Front views of the macrocycles; views in all compounds approximately along the N−N axis indicated by the arrows in the left column. Right column: Out-of-plane displacement plots of the bacteriochlorin macrocycles. The RMSD values listed are of the $C_{16}N_4$ bacteriochlorin chromophore.[30] The white asterisk in the plot for **11a** indicates the morpholine carbon linked to the neighboring *meso*-phenyl group.

as 5^{Ar}**b**, with Ar = *p*-tolyl; RMSD value of 0.176 Å).[27b,c,30] Evidently, the bacteriochlorin chromophore is more flexible than the chlorin chromophore and therefore responds much more strongly to the strain introduced by the insertion of the oxygen atom between the two sp³-hybridized pyrroline *β*-carbons. The increase of the flexibility of porphyrinoid macrocycles with increasing saturation is well described.[6a,31]

Treatment of morpholinobacteriochlorin 10^{Ar} with acid leads to the establishment of an intramolecular *β*-to-*o*-phenyl linkage. This intramolecular Friedel−Crafts-type reaction is equivalent to that observed in the morpholinochlorin series,[27c,33] except that two diastereomers are formed, **11a** and **14** (each as a pair of enantiomers), that vary in the relative position of the new linkage with respect to the dihydroxy functionality on the opposite pyrroline; they could be on opposite sides of the plane defined by the macrocycle (*E*-arrangement), or the same side (*Z*-arrangement). A single crystal structure of the majority compound **11** confirms the *anti*-arrangement of the link to the phenyl group and the alkoxy group on the morpholine ring, the relative *E*-arrangement of the link and the dihydroxy

functionality on the opposite pyrroline, the near-*co*-planar arrangement of the linked *meso*-phenyl group with the porphyrinoid chromophore, and the introduction of nonruffled out-of-plane conformational modes (some mild doming and saddling can be made out) (Figure 1).[5b]

The methodology to expand a dihydroxypyrroline to a dialkoxymorpholino moiety can also be applied twice on the same molecule, as the conversion of the tetrahydroxybacteriochlorins 4^{Ar} to bismorpholinobacteriochlorins 12^{Ar} demonstrates. The NMR spectra of 12^{Ar} are much simplified, indicative of their high symmetry. The crystal structure of **12** highlights how the twists within each six-membered morpholine subunit translate into a ruffling of the chromophore, whereby the handedness of the twists of the morpholine moieties are complementary to each other. The helical chromophore conformation determines through steric and stereoelectronic effects the absolute stereochemistry of both alkoxy substituents on each morpholine unit.[27c] Thus, only one racemic pair of **12** is formed, irrespective of the presence of five

chiral elements—four chiral centers and a chiral axis. The structure of 12^{CF_3} is near-identical to that of **12** (see the SI).

Treatment of bismorpholinobacteriochlorins 12^{Ar} with traces of TFA vapors generated new compounds with a composition that indicated that a loss of two MeOH groups had taken place, suggestive of the formation of two *β*-to-*o*-phenyl-linkages. The NMR spectra of products 13^{Ar} showed the formation of 2-fold symmetric molecules. The absence of detectable diastereomers and an extension of the general tight stereochemical coupling between the macrocycle helicity and the stereochemistry of the substituents allowed us to predict that 13^{Ar} is the result of two unidirectional *β*-to-*o*-phenyl-fusion reactions with the relative stereochemistry shown, but a solid state structure conformation remained elusive. Precedence in similarly bis-modified bacteriochlorins,[34] and, as we will demonstrate below, the successful computational modeling of the optical spectrum of **13** further supports its regio- and stereochemistry as shown.

Optical Properties of the Morpholinobacteriochlorins. Bacteriochlorins of the type 4^{Ar} (or their alkylated versions 6^{Ar} or 9^{Ar} in either *E* or *Z* configurations) possess regular bacteriochlorin UV−vis spectra (Figure 2A). We have assigned
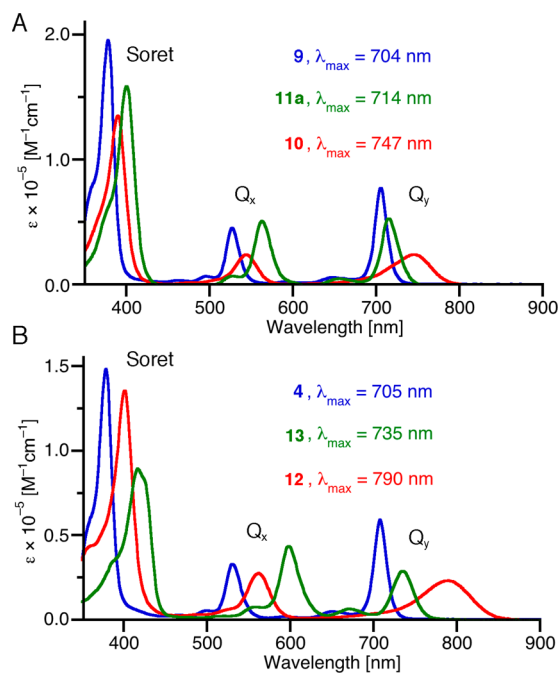

Figure 2. UV−vis spectra (CH_2Cl_2) of the compounds indicated.

the Soret, Q_x and Q_y ($λ_{max}$) bands according to the standard Gouterman model.[11] Expansion of one pyrroline moiety to a morpholine in **10** causes a substantial bathochromic shift (42 nm of the Q_y transition), and overall broadening of its UV−vis spectrum that retains bacteriochlorin character. The red-shift is more significant than the corresponding shift observed in the chlorin 3^{Ar}-to-morpholinochlorin 5^{Ar} conversion,[27b] likely the result of the larger degree of nonplanarity that this modification introduces into the bacteriochlorin chromophore.[35] The spectral broadening suggests a significant conformational flexibility of the chromophore.

The establishment of the *β*-to-*o*-phenyl-fusion in **11a** leads to a blue-shift of the Q_y band compared to the spectrum of its parent compound **10**, but curiously to a red-shift of the Soret and the Q_x bands. On account of the extended *π*-conjugation of

the porphyrinic chromophore, the optical spectra of most porphyrinoids that incorporate such motifs are red-shifted compared to the parent chromophore.[36] That this is not observed here suggests that conformational effects may have overridden the extended *π*-conjugation effects. Calculations presented below support this view. The *β*-to-*o*-phenyl-link presumably also increases the conformational rigidity of the chromophore, rationalizing the overall sharpening of the optical spectrum.

The trends described for the monomorpholinobacteriochlorins also hold for the bismorpholinobacteriochlorin series (Figure 2B): The conversion of two pyrrolines to generate 12^{Ar} results in a pronounced red-shift of all bands (85 nm for the Q_y) and a broadening of the spectrum. Correspondingly, the conformation of **12** is also severely nonplanar. A double *β*-to-*o*-phenyl-fusion in **13** blue-shifts $λ_{max}$ and red-shifts the Soret and Q_x bands. Even though the solid state structure of this compound is not known, it can be predicted to be more planar than **12**; calculations presented below will confirm this.

Calculated Structures of the Morpholinobacteriochlorins. To investigate the native conformations of the tetramethoxybacteriochlorin and mono- and bis-morpholinobacteriochlorin macrocycles unaffected by, for example, crystal packing effects, we minimized their geometries using a well benchmarked DFT method for hydroporphyrinoids (B3LYP/6-31g(d)), with and without solvent (CH_2Cl_2) (Table 1). A number of observations are noteworthy. The fully minimized structures of **6-Z** and **10** deviated only minimally from their solid state structures (deviations of the RMSD values of the calculated and experimental structures <0.05 Å).[24] Thus, the gauche-conformation of the two alkoxy groups in the crystal and computed structures of **6-Z** were virtually identical (28.5° versus 28.9°, respectively). A major difference with the experimental conformation is observed for bismorpholinobacteriochlorin **12**. The computed structure is significantly more ruffled than the experimental structure,[7b] with a computed RMSD value of nearly 0.2 Å higher than the experimental value. We will demonstrate that the computed structure more likely represents the solution state conformation. The discrepancy of the solid and solution state conformations suggests a low-energy conformational barrier for this molecule, as also demonstrated computationally below.

The energy minimizations of the monofused morpholinobacteriochlorin **11a** provided qualitatively similar conformations as observed in the crystal structure, with only a minimal (~0.04−0.05 Å) overall larger out-of-plane distortion. This structure, together with the computed structure of bis-linked morpholinobacteriochlorin **13**, will be discussed in detail below.

Calculated Optical Spectra of the Morpholinobacteriochlorins. All five bacteriochlorins **4**, **10**, **11**, **12**, and **13** contain identical 18 *π*-electron $C_{16}N_4$ chromophores, substituted by *meso*-phenyl groups and sp^3-carbon atoms, but of varying conformations. The two morpholinobacteriochlorins **11** and **13** containing *β*-to-*o*-phenyl-fusions represent chromophores in which a mix of major electronic influences (*π*-extension) and conformational effects determine their optical properties. We therefore will discuss the computed electronic structures of the two groups of compounds separately from each other, beginning with the nonfused systems; the discussion of the fused systems is reserved for the end of this report.

We computed the optical spectra of the three bacteriochlorins **4**, **10**, and **12** in their solid-state conformations[7b,24] (in

Table 1. Comparison of Macrocycle Nonplanarity and Q-Band Wavelengths for the Computed and Experimental Solution State Spectra of the Compounds Indicated

structure	RMSD (Å)[b]	calcd absorption wavelengths (nm)[a]		exptl absorption wavelengths (nm)	
		Q_x	Q_y	Q_x	Q_y
4 (in crystal conformation of 4$^{(OMe)_3}$-Z)[c]	0.141	541	648		
4 (DFT, vacuum)	0.092	540	671		
4 (DFT, CH$_2$Cl$_2$)	0.098	562	737		
4 (CH$_2$Cl$_2$)				524	707
10 (in crystal conformation of 10^{CF_3})	0.364	556	707		
10 (DFT, vacuum)	0.332	570	726		
10 (DFT, CH$_2$Cl$_2$)	0.340	595	801		
10 (CH$_2$Cl$_2$)				542	742
12 (in crystal conformation of 12)	0.293	556	718		
12 (DFT, vacuum)	0.464	598	775		
12 (DFT, CH$_2$Cl$_2$)	0.466	625	855		
12 (CH$_2$Cl$_2$)				562	790
11 (in crystal conformation of 11a)	0.277	572	672		
11 (DFT, vacuum)	0.315	583	686		
11 (DFT, CH$_2$Cl$_2$)	0.325	618	746		
11 (CH$_2$Cl$_2$)				563	715
13 (DFT, vacuum)	0.421	619	698		
13 (DFT, CH$_2$Cl$_2$)	0.429	663	755		
13 (CH$_2$Cl$_2$)				598	735

[a]Calculated using TD-wB97XD/6-31+g(d) on, using B3LYP/6-31g(d), fully minimized structures. [b]Root mean square deviation of the C$_{16}$N$_4$ macrocycle that excludes all pyrroline and morpholine β- and O-atoms. [c]CCDC 756649. The solid-state structure has hydroxyl, instead of methoxy substituents, and 3,4,5-trimethoxyphenyl groups, instead of phenyl groups, but it is known that none of these differences have an appreciable effect on the absorption properties.[24]

the absence of all solvents and, where present, having replaced all *meso*-aryl groups with *meso*-phenyl groups) and in their DFT minimized conformations using TD-DFT (wB97XD/6-31+g(d)) (Table 1, Figure 3).[37] Details of the minimization procedures used here and throughout the paper are given in the
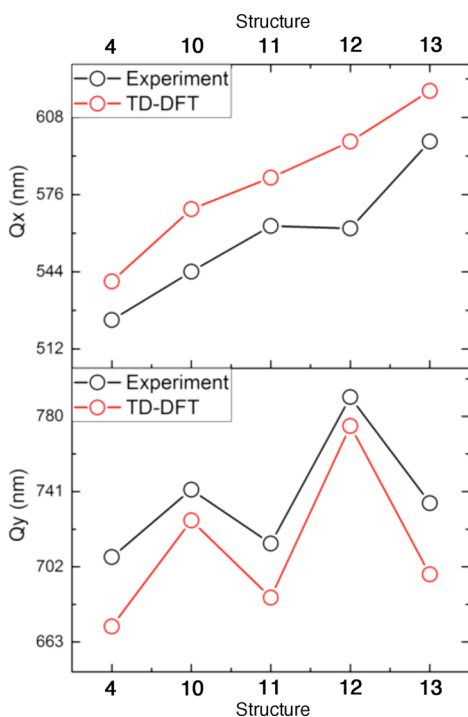
Figure 3. Illustration of the faithful reproduction provided by TD-DFT of the experimental Q$_x$ and Q$_y$ wavelength trends for all expanded bacteriochlorins studied.

SI. Calculations were done in vacuum and with implicit solvent (CH$_2$Cl$_2$) using the conductor-like polarizable model (CPCM)[38] as implemented in Gaussian 09.[39] TD-DFT has been used to successfully describe the optical properties of a variety of porphyrinic systems, including recently also for 12.[10d] Computed trends were given a heavier weight than absolute numbers.

Overall, the validity of our TD-DFT computed spectra is underscored by the faithful reproduction of the experimental spectral trends for the principal molecules of this study (Figure 3). The origin and orbital composition of the Q$_x$ and Q$_y$ transitions are presented in the SI.

Experimentally, with each conversion of a pyrroline to a morpholine subunit, the Q$_x$ and Q$_y$ transitions are observed to shift bathochromically by 18−20 nm and 38−42 nm, respectively. Spectral shifts consistent with these trends (Q$_x$: 28−33 nm, Q$_y$: 49−64 nm) were only obtained for the fully minimized (vacuum or implicit solvent) geometries. Notably, the spectrum of the computed structure of bismorpholino-bacteriochlorin 12 is in much better agreement with the experimentally observed optical data than the spectrum based on the solid state structure. This confirms the supposition that the unusually little ruffled conformation of 12 seen in the crystal structure does not reflect its equilibrium geometry in solution.[7b] While the inclusion of implicit solvation resulted in quantitatively different absorption wavelengths, it consistently reproduced the trends obtained in the vacuum calculations (see the SI). Thus, for the remainder of this discussion, we rely exclusively on calculated vacuum spectra.

Structure-Optical Properties Correlations. The correct reproduction of the spectra allowed us to interrogate the morpholinobacteriochlorin chromophores with respect to the structural origins of the observed large spectral-shifts. We followed a series of steps to untangle the contributions to the

spectral shifts: (1) The direct electronic role of the ring oxygen(s) was investigated by stepwise replacement with sp^3-hybridized carbon atoms. (2) The effect of ruffling was investigated by mutating the morpholinobacteriochlorins to the parent tetrahydroxybacteriochlorins, leaving the distortions of the chromophore intact. (3) The effects of localized morpholine distortions were finally resolved and analyzed.

With the principal effect identified, we then explored (4) the conformational landscape of a morpholinobacteriochlorin in regard to the thermally accessible $C_\beta–C_\alpha–C_\alpha–C_\beta$ dihedral angles, and (5) detailed the metrics of the localized perturbation of the macrocycle upon the insertion of one or two oxygen atoms. Lastly, we investigated the electronic and conformational influence of the β-to-o-phenyl linkages. In all cases, we calculated the electronic consequences of the perturbations, and compared the results to each other and the experimental findings. This strategy of analyzing conformation-induced spectral modulations by optimizing and examining perturbed structures is broadly accepted.[5f,7c,40]

Role of the Morpholine Oxygen. Dihydroxylation of the pyrroline β-positions of a bacteriochlorin is known to cause a 16−18 nm hypsochromic shift of the λ_{max} (Q_y) band.[24] Conceivably, therefore, further oxidation of the β-position(s) could induce an additional blue shift, perhaps even mitigating the bathochromic shifts originating from conformational distortions. To test this hypothesis, the morpholine ring O atom in the minimized morpholinobacteriochlorin **10** was substituted by a methylene (CH_2) moiety (**10** → **10^C**). Only this replacement moiety in the fictive molecule was minimized, the spectrum computed, and the results were compared to the corresponding spectra of the parent compound (Table 2). This

Table 2. Electronic Influence of the Morpholine Oxygen on the Q-Band Wavelengths Delineated through CH_2 Substitution
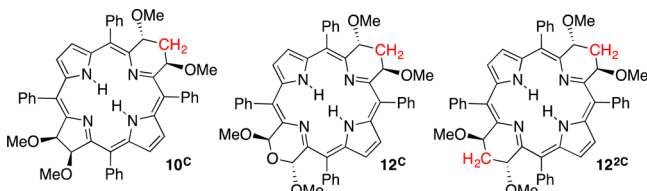
structure	exptl	calcd[a,b]	exptl	calcd[a,b]
10	524	570	745	726
10^C		567		724
12	540	598	790	775
12^C		595		772
12^{2C}		593		771

[a]Only the methylene fragments of these structures were optimized; the rest of the structure was fixed in the optimized geometry prior to the modification. [b]Calculated using the TD-wB97XD/6-31+g(d) model.

procedure was also applied twice in a stepwise fashion to bismorpholinobacteriochlorin **12** (**12** → **12^C** → **12^{2C}**). Overall, the electronic effects of this substitution were minimal, producing only ~1−4 nm batho- or hypsochromic shifts of the Q_x and Q_y bands.

We thus conclude that the introduction of the ring-O atom exerts only a minimal electronic effect on absorption properties of the morpholinobacteriochlorins. Therefore, the spectral

modulation observed upon pyrroline expansion of a bacterio-chlorin appears to be primarily of conformational origin.

Role of the Ruffled Conformation. Past studies of tetrapyrrolic chromophores indicated that macrocycle non-planarity is a key structural factor impacting their electronic properties.[5h,7a,41] To quantify the effects of out-of-plane distortions of the bacteriochlorin $C_{16}N_4$ chromophore, we computed regular bacteriochlorin **4** in the locked conforma-tions of its morpholinobacteriochlorin analogues **10** (referred to as conformer **4^{morph}**) and **12** (conformer **4^{bismorph}**). The UV−vis spectra were then computed for all compounds (Table 3).

Table 3. UV−Vis Spectral Influence of Macrocycle Nonplanarity

| structure | calcd absorption wavelengths (nm)[a] | |
	Q_x	Q_y
4	540	671
4^{morph}	557	691
4^{bismorph}	572	704
10	570	726
12	598	775

[a]Calculated using the TD-wB97XD/6-31+g(d) model chemistry. Only structures **4**, **10**, and **12** were fully minimized. Structures **4^{morph}** and **4^{bismorph}** were derived from **10** and **12**, respectively, as described in the text and SI.

For the ruffled bacteriochlorin conformers **4^{morph}** and **4^{bismorph}**, a substantially smaller bathochromic shift was predicted than computed or observed for **10** and **12**, respectively (Table 1). For instance, a 55 nm shift for the Q_y transition was predicted to be associated with the trans-formation **4** → **10**, and an additional 48 nm shift of the Q_y for the transformation **10** → **12**. However, for the transformations **4** → **4^{morph}** and **4** → **4^{bismorph}**, only 20 and 13 nm shifts were computed, respectively. Comparable findings apply to the Q_x transitions.

Thus, macrocycle nonplanarity accounts for a significant fraction of the observed bathochromic shifts of the Q_y and Q_x transitions, but is not responsible for *all* of the shifts observed. We therefore conclude that other structural factors than chromophore nonplanarity must be at play to rationalize the large red-shifts of the morpholinobacteriochlorins. This finding parallels the study of nonplanar porphyrins,[41] but as we will demonstrate, the other contributing factor is unique to the morpholinobacteriochlorins.

One ancillary feature of the conformer series **4** → **4^{morph}** → **4^{bismorph}** is that the energetics of the macrocycle conformational distortion are directly comparable. The distortion of near-planar **4** to ruffled **4^{morph}** is associated with an ~7.5 kcal/mol energetic cost; further distortion to the conformation of **4^{bismorph}** indicates an additional energetic penalty of ~9.3 kcal/mol (Figure 4 and SI). The energetic costs of deforming the aromatic systems from planarity are therefore, as expected, nonlinear, and increase faster as the distortion becomes larger.

*Effects of Morpholine Torsional Distortion.* Since the bacteriochlorin macrocycle nonplanarity induced by the insertion of an oxygen into the pyrrolines accounts for only a fraction of the experimentally observed bathochromic shift of the morpholinobacteriochlorin spectra, and the oxygen substitution itself has only a minimal effect, we explored other mechanisms that might have contributed to the observed
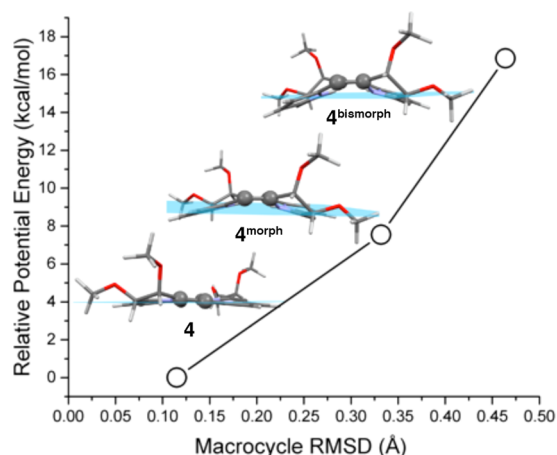
Figure 4. Relative conformational energetics of the ruffling of the bacteriochlorin chromophore **4**.

spectral modulations. Two peripheral perturbation mechanisms were explored (Figure 5). First, the pyrroline of the minimized
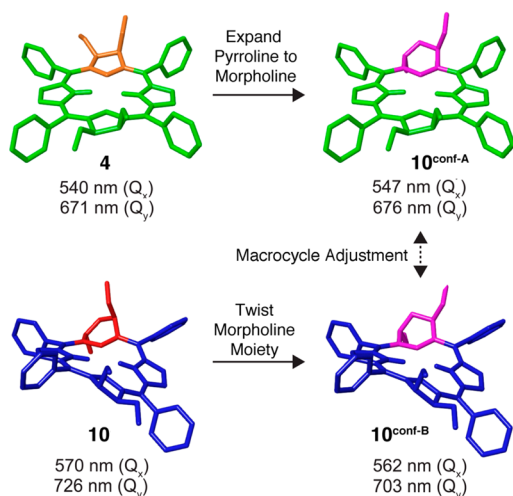
Figure 5. Hypothetical stepwise pyrroline-to-morpholine conversion that dissects the various structural contributions to the spectral modulation of morpholinobacteriochlorins. Only **4** and **10** were fully minimized; **10**[conf-A] and **10**[conf-B] were derived as described in the text and SI from these minimized structures.

tetramethoxybacteriochlorin **4** was expanded by oxygen insertion and the saturated portion of the morpholine moiety was relaxed, while the conformation of the rest of the structure was retained (**4** → **10**[conf-A]). Second, we adjusted the C_β–C_α–C_α–C_β dihedral of the fully minimized structure of morpholinobacteriochlorin **10** to the value observed in **10**[conf-A], and minimized the C_β–O–C_β portion of the morpholine while holding the rest of the molecule fixed (**10** → **10**[conf-B]). This procedure provides two conformers of **10** (**10**[conf-A] and **10**[conf-B]) with identical morpholine C_β–C_α–C_α–C_β dihedral angles (20.4°), but that differ in the degree of nonplanarity of the remainder of the macrocycle. The Q_x and Q_y transition wavelengths of all conformers were computed.

The structural changes are associated with characteristic shifts of the computed absorption bands: The Q_x and Q_y bands of **10**[conf-A] are only marginally (7/6 nm) red-shifted when compared to those of **4**, thus the structural changes to accommodate the oxygen had little effect. Larger (15/27 nm)

shifts for the Q_x and Q_y bands, respectively, are associated with the increase of nonplanarity of the chromophore; they are in the same order of magnitude as observed for the adjustment of the chromophore in the absence of the morpholine moiety, detailed above. The real surprise is the additional 8/23 nm shifts for the Q_x and Q_y bands, respectively, upon adjustment of the morpholine C_β–C_α–C_α–C_β dihedral angle (from 20.4° for **10**[conf-B] to 43.3° for **10**).

In fact, a linear relationship between dihedral angle and Q_y optical transition shift can be derived, while the Q_x band shifts are somewhat less linear and follow a different proportionality (Figure 6). For the Q_y band, a bathochromic shift of ∼2 nm/° twist is predicted in the range of the C_β–C_α–C_α–C_β dihedral angle between 25 and 50°. The effects of two successive ring-expansions are additive (see the SI). Importantly, the sum of the shifts derived from the macrocycle deformation and the increase of the morpholine C_β–C_α–C_α–C_β dihedral angles add up to the computed shift from **4** to **10** (or **10** to **12**), and which are only marginally more than the overall shift observed experimentally. Each component is responsible for ∼50% of the computed shift. We will show below that this relationship can also predict the optical shifts observed for the *meso*-linked morpholinobacteriochlorins of type **11** and **13**.

The modulation of the torsional distortion of a nonpyrrolic subunit within a porphyrinic chromophore is a hitherto unidentified mechanism for the spectral tuning of bacterio-chlorin chromophores. This mechanism likely has more general implications for other ring-expanded hydroporphyrinoids in which the C_β–C_α–C_α–C_β dihedral angle can be adjusted.[42]

Potential Energy Surface (PES) Profile of the Morpholine Torsional Distortion. To further illuminate the spectral effect of the twisting of the C_β–C_α–C_α–C_β torsion angle within the morpholine subunit (**10**[conf-B] → **10**), a relaxed potential energy surface (PES) scan over the C_β–C_α–C_α–C_β morpholine torsion angle in **10** within the readily thermally accessible range of ±1 kcal/mol around the minimum was performed. Excited state properties were calculated at each point of the scan (Figure 6C). The PES profile of morpholinobacterio-chlorin **10** is asymmetric, with a greater number of conformers within 1 kcal/mol of the minimum possessing smaller morpholine C_β–C_α–C_α–C_β torsional angles than larger angles. The thermally accessible distribution of conformers qualitatively agrees with the experimental asymmetry of the absorption bands of **10** and **12** (Figure 2). The degree of the distortion is directly correlated to the extent of the optical shift (Figure 6A). Relative to the fully optimized structure (with a 43.3° angle), the Q_y band of the less twisted conformers exhibits a hypsochromic shift, while the more twisted structures exhibit a bathochromic shift. The modulation of the morpho-line C_β–C_α–C_α–C_β dihedral angle imposes, however, only minor effects on the remainder of the macrocycle (Figure 6B). The maximum increase in the macrocycle RMSD among the conformers shown is 0.024 Å. This small change indicates that substantial twisting of this portion of the macrocycle can take place essentially independently from the remainder of the chromophore, a conclusion further supported by more detailed metric analyses.
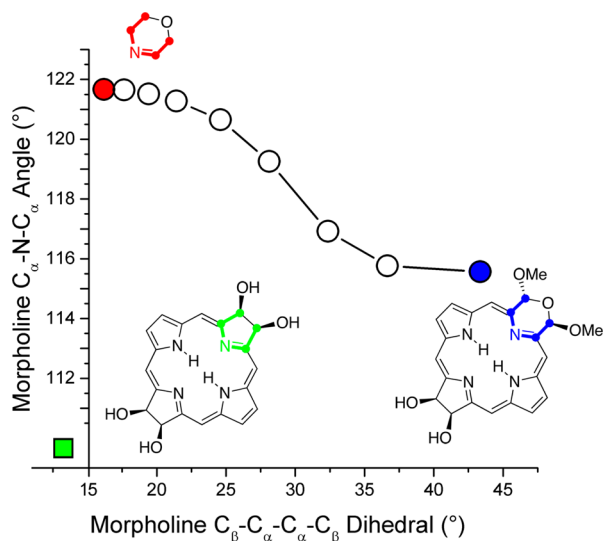
Metric Analysis of the Structural Effects of the Pyrroline Ring Expansion. We further analyzed the structural effects of the pyrroline ring expansion on the remainder of the macrocycle to identify the atoms within the π-aromatic chromophore that are most affected by this perturbation. Conversion of a pyrroline to a morpholine (**4** → **10** or **10** →
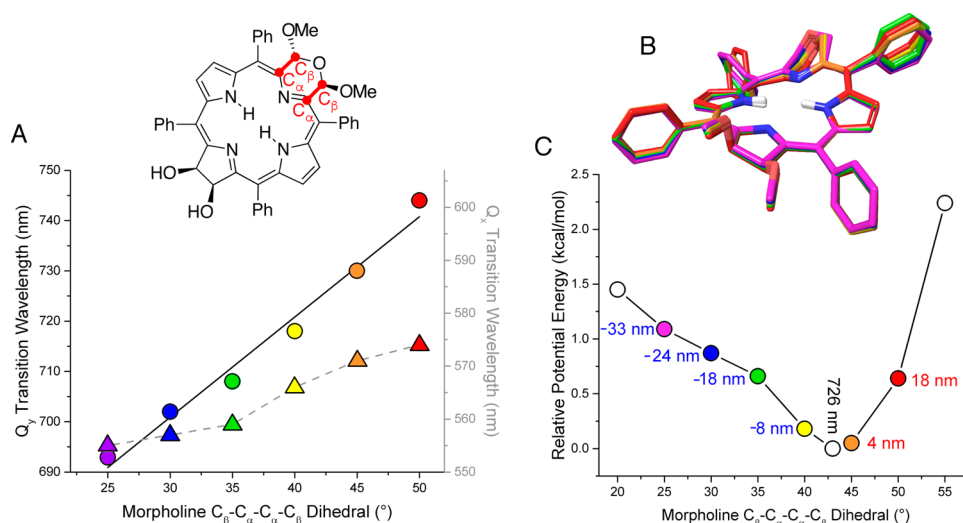
Figure 6. (A) Modulation of the Q_x and Q_y wavelengths as a function of the $C_\beta-C_\alpha-C_\alpha-C_\beta$ dihedral in the conformers of morpholinobacteriochlorin **10** shown. The trend-line for the Q_y bands is indicated in black and fits the following equation: TD-DFT Q_y wavelength = 640($\pm$5) nm +2.0($\pm$0.1)/deg torsion angle. The regression analysis has a R^2 of 0.98, whereas the gray line for the Q_x band relationship simply connects the points. The colors of the spots represent the conformations of **10** shown in (B). (B) Superposition of conformers of morpholinobacteriochlorin **10** within $\pm$1 kcal/mol of the minimum. The methoxy substituents on the morpholine moiety were included in the computations but were omitted here for clarity. (C) Relaxed PES scan of morpholinobacteriochlorin **10** over the dihedral angles indicated and the associated Q_y wavelength shifts (hypsochromic, blue; bathochromic, red) relative to the wavelength for the fully relaxed geometry.

12) results in a 6° enlargement of the $C_\alpha-N-C_\alpha$ angle of the expanded subunit (from 109° to 116°). However, the corresponding angle in free 1,2-dehydromorpholine is ~122° (Figure 4). Hence, the $C_\alpha-N-C_\alpha$ bonds in the morpholino-bacteriochlorins are strained. Likewise, isolated 1,2-dehydro-morpholine has a $C_\beta-C_\alpha-C_\alpha-C_\beta$ dihedral angle that is ~30° smaller than that found in the morpholine moieties within **10** (or **12**). Our modeling studies found that, in morpholino-bacteriochlorin **10**, the compression of the morpholine $C_\alpha-N-C_\alpha$ angle is directly countered by a $C_\beta-C_\alpha-C_\alpha-C_\beta$ dihedral increase (Figure 7).

Another interesting feature is the relatively localized nature of the distortions within the $C_{16}N_4$ chromophore observed upon insertion of the oxygen atom(s) into a regular bacteriochlorin (i.e., the conversions **4** → **10** → **12**) (Table 4). The metric changes observed in the bond angles and dihedrals closest to the oxygen insertion site are twice or even four times larger in almost every instance than the changes on the distal side.

In general, distortions that affect π-orbital overlap will modulate the spectral properties. For instance, distortions of the C_α-C_{meso} angles from the (presumably ideal) angles found in regular porphyrins have been shown to induce bathochromic shifts in these nonplanar porphyrins.[5f,43] The largest localized distortions involving the C_α, C_β, or C_{meso} atoms are therefore suggested to be primarily responsible for the spectral modulation observed upon the formation of mono- and bismorpholinobacteriochlorins.

Evaluation of the Phenyl-Fused Morpholinobacterio-chlorins. To computationally assess the spectral effect of the β-to-o-phenyl linkage, we broke the linkage in the minimized structure of **11**, saturated the open valences with hydrogen atoms, and arranged the affected *meso*-phenyl group perpendicular to the mean plane of the chromophore (Figure 8, **11** → **15**). The resulting optical spectra were computed and compared. Relative to the hypothetically unlinked structure **15**, the spectrum of **11** indicated that the Q_x band had red-shifted by a surprising 30 nm, while the Q_y band red-shifted only 9 nm. A repetition of the calculations with bis-linked structure **13** showed an additive shift of these amounts per linkage (see the SI). These shifts thus represent the value for the increased π-conjugation of the bacteriochlorin chromo-phore with a near-*co*-planar phenyl group. Even though porphyrinoids with β-to-o-phenyl linkages are well-known,[36] including the finding that they are generally characterized by red-shifted optical spectra, we are not aware of a report in which the value of the expanded π-conjugation was determined
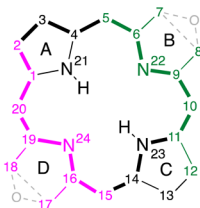

Figure 7. Depiction of the conformational link between the ruffling of a morpholino moiety, as expressed as the $C_\beta-C_\alpha-C_\alpha-C_\beta$ dihedral, and the compression/expansion of its $C_\alpha-N-C_\alpha$ angle. *meso*-Phenyl groups were included in the computations, but are omitted here for clarity. Colored symbols refer to the dihedral values found in the fully minimized structures indicated.

Table 4. Computed Torsional Angles in 4, 10, and 12, and Angle Changes Induced by the Pyrroline-to-Morpholine Conversions

Dihedral Angle[a]	4	|Δ 4-10|	10	|Δ 10-12|	12
5-6-N-9	178.6	17.4	-164.1	1.9	-166.0
6-N-9-8	9.8	18.2	28.0	2.1	30.1
6-N-9-10	-172.3	17.1	-155.2	2.8	-152.4
7-6-9-8	13.3	30.0	43.3	0.3	43.0
7-6-N-9	4.1	16.5	20.6	2.5	18.2
N-9-10-11	-5.2	3.6	-8.8	1.3	-7.5
8-9-10-11	172.5	4.6	167.9	1.9	169.8
9-10-11-12	-179.2	17.3	163.5	4.4	159.1
15-16-N-19	172.3	9.9	-177.8	22.7	-166.1
16-N-19-18	-4.1	15.4	11.3	18.9	30.1
16-N-19-20	-178.6	11.4	-167.2	4.8	-152.4
17-16-19-18	-13.3	29.1	15.8	27.2	43.0
17-16-N-19	-9.8	15.0	5.2	12.9	18.1
N-19-20-1	-5.2	6.1	0.9	8.4	-7.5
18-19-20-1	-179.1	1.6	-177.5	12.6	167.0
19-20-1-2	177.5	8.8	168.7	9.6	159.1

[a]For better overview, the bonds involved are grouped and color-coded. Because of the idealized 2-fold symmetry of the ruffled molecules, only half of the possible dihedral angles associated with the morpholine moieties are listed.
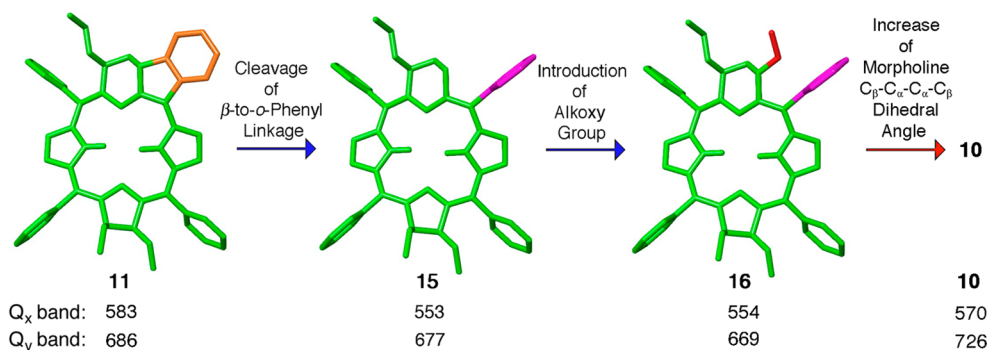
Figure 8. Hypothetical stepwise transformation of β-to-o-phenyl linked morpholinobacteriochlorin into a conformer of the unlinked analogue. The green portion of each structure is unchanged in each step. Structures **15** and **16** were derived from fully minimized **11** as detailed in the main text and SI. Wavelengths listed correspond to TD-DFT-calculated values for the species indicated.

for compounds of otherwise identical chromophore conformation.

Notwithstanding the bathochromic effect of π-extension, a β-to-o-phenyl linkage is computed to cause a 40 nm blue-shift (27 nm found experimentally) for the Q_y transition. The origin of the overall blue-shift observed upon realization of the β-to-o-phenyl linkage(s) in **11** (or **13**) is complicated by the absence of an alkoxy group per linkage. As β-alkoxy substituents are known to have a significant inductive hypsochromic effect on the Q_y transition,[24,27c] their replacement with an aryl linkage is expected to cause a red-shift. Consistent with this expectation, we find that structure **15** (corresponding to **16** lacking the OMe group), has a computed Q_y transition that is 8 nm red-shifted relative to structure **16**; the Q_x transition is not significantly affected. Thus, the resonance-induced red-shift for the Q_y transition upon β-to-o-phenyl linkage described above was underestimated by ~8 nm. Since the combined electronic effects of replacing a β-alkoxy group with a β-to-o-phenyl linkage on the Q_y transition is computed to be an ~17 nm (9 + 8 nm) red-shift, we submit that conformational effects override the substituent-induced electronic effects to result in the significant blue-shift computed (40 nm) and observed (28 nm) for Q_y upon establishment of the β-to-o-phenyl linkage (Figure 8). The linkage planarizes the macrocycle and particularly the

morpholine moiety (cf. Figure 1). Both changes were above shown to cause a blue-shift. We observe from Table 1 that the fully minimized crystal structure of monofused **11** is only ~0.02 Å more planar than fully minimized morpholinobacteriochlorin **10**. Macrocycle planarization, therefore, is expected to have only a minor effect. However, the $C_\beta-C_\alpha-C_\alpha-C_\beta$ dihedral angle is reduced from 43.3° in regular morpholinobacteriochlorin **10** to 13.9° in monofused **11**. From the torsion angle-Q_y wavelength relationship derived (Figure 6), we can predict that a morpholinobacteriochlorin with an ~14° $C_\beta-C_\alpha-C_\alpha-C_\beta$ dihedral angle would correspond to a Q_y wavelength between 668 and 673 nm. The TD-DFT computed Q_y wavelength for fully minimized monofused **11** is 686 nm. Thus, subtracting the ~17 nm red-shift from electronic substituents effects, we obtain a predicted Q_y wavelength for monofused **11** of 669 nm, in excellent agreement with the prediction from the analysis of the effects of the morpholine $C_\beta-C_\alpha-C_\alpha-C_\beta$ dihedral angle.

We therefore conclude that the planarization of the morpholine moiety by 29° is the main cause for the remarkable 58 nm blue-shift of the Q_y transition, mitigated by a 17 nm red-shift due to the summed-up electronic effects of β-to-o-phenyl linkage. More generally, this underscores again that the morpholine $C_\beta-C_\alpha-C_\alpha-C_\beta$ dihedral angle is a major

determinant in the optical properties of the morpholinobacteriochlorin chromophores. Furthermore, when other substituent effects are also considered, this angle provides a reliable estimation of the Q-band absorption wavelength.

CONCLUSIONS

The elucidation of the components of the structural origins of the large red-shifts of the Q-bands observed upon pyrroline-to-morpholine conversions in bacteriochlorins is found to be a function of two major factors: molecular planarity and the $C_\beta-C_\alpha-C_\alpha-C_\beta$ dihedral of the morpholine moiety. Each variable contributes about half of the observed shifts. The influence of the degree of nonplanarity on the $C_{16}N_4$ chromophore was expected but the observation that the $C_\beta-C_\alpha-C_\alpha-C_\beta$ dihedral of the morpholine moiety is an additional important factor was not. However, clear relationships between this dihedral angle and the resulting shifts of the Q_x and particularly the Q_y bands (2 ± 0.1 nm/° twist) can be derived. Both factors are also largely independent from each other as the modulation of the morpholine moiety dihedral angle has only a relatively local effect on the conformation of the macrocycle.

Other types of local torsional distortions were also surmised to be operative in the optical modulation of the *c*- versus *d*-type bacteriochlorins (that, despite their naming, belong to the chlorins), photosynthetic accessory pigments found in the *Chlorobiaceae* and *Chloroflexaceae*. The *c*-series vary from the *d*-series by the presence of a *meso*-methyl group. X-ray diffractometry studies of the model [13^1-deoxophytoporphyrinato]nickel(II) complexes **17** and **18** found structural evidence for this.[4] Also, the origin of the red-shift observed in ruffled *meso*-substituted porphyrins, such as **19M**, has been attributed to localization of the nonplanar distortion in dihedrals centered around $C_\alpha-C_{meso}$ bonds.[5f,43]

17, R = H
18, R = Me

19Zn, M = Zn(II)
19Ni, M = Ni(II)
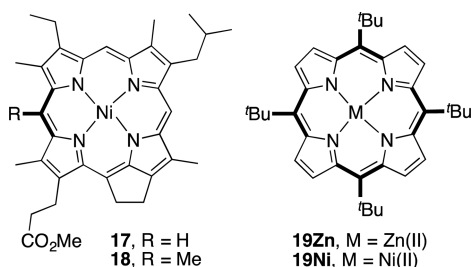
An in-depth understanding of the structural origins of the physicochemical modulation of bacteriochlorin analogues is essential for the rational and application-oriented design. We are adding herewith a previously unrecognized mechanism to the canon of structural tools for the modulation of porphyrinoid chromophores that allow a modulation of the $C_\beta-C_\alpha-C_\alpha-C_\beta$ dihedral angle. Moreover, the morpholine $C_\beta-C_\alpha-C_\alpha-C_\beta$ dihedral angle can also serve as an excellent predictive tool to estimate the conformationally induced shifts of the optical spectra of bacteriochlorins and bacteriochlorin analogues. However, unlike many pyrrole-modified porphyrins incorporating either larger than 5-membered (partially saturated) heterocycles or cleaved $\beta-\beta'$-bonds, it should be noted that porphyrins and regular hydroporphyrins are likely resistant to this optical modulation. This work also highlights the large conformational flexibility of the morpholinobacteriochlorins.

The strong conformational influence of the optical properties of the morpholinobacteriochlorin chromophores (and, by extension, also the related morpholinochlorins, thiamorpholinochlorins, and other hydroporphyrin analogues with flexible nonpyrrolic building blocks),[8,9b] combined with their significant conformational flexibility, suggests these dyes for mechanochromic applications.[44] Experiments toward this goal are currently ongoing in our laboratories.

EXPERIMENTAL SECTION

Materials. The preparations of all compounds are described in detail in the SI, including a reproduction of all NMR and UV−vis spectra.

Computations. All partial and full ground state geometry optimizations were performed with the Becke, three-parameter, Lee−Yang−Parr (B3LYP) hybrid functional,[45] a 6-31g(d) basis set, and an ultrafine grid for integration, as implemented in Gaussian 09 revision D.01.[39] This model has been recommended for hydroporphyrins.[6c,10c] Vertical excitations were calculated with time-dependent DFT (TD-DFT) at the wB97XD/6-31+g(d) level of theory. Mazzone et al. recently showed that the combination of these two levels of theory can quantitatively reproduce the vertical transition wavelengths for **4**, **10**, and **11−13**.[10d]

X-ray Single Crystal Diffractometry. Details of the data collection and structural parameters for the structure elucidation of **12^{CF_3}**, including CIF files, descriptions of disorder and hydrogen atom treatment, and software packages used, can be found in the SI. The crystallographic data, in CIF format, have been deposited with the Cambridge Crystallographic Data Centre under number CCDC 1510280. These data can be obtained free of charge from The Cambridge Crystallographic Data Centre via www.ccdc.cam.ac.uk/data_request/cif.

ASSOCIATED CONTENT

ⓈSupporting Information

The Supporting Information is available free of charge on the ACS Publications website at DOI: 10.1021/jacs.6b12419.

> Reproduction of the UV−vis, ^{1}H and ^{13}C spectra of all novel compounds, experimental details for the crystal structure determinations, Cartesian coordinates of calculated structures, and additional computational details (PDF)
> Crystal data for **12^{CF_3}** (CIF)
> PDB files of computed structures (ZIP)

AUTHOR INFORMATION

Corresponding Authors
*rbirge@uconn.edu
*jose.gascon@uconn.edu
*c.bruckner@uconn.edu

ORCID Ⓞ
Christian Brückner: 0000-0002-1560-7345

Present Address
‖M.Z.: Department of Chemistry, Purdue University, 101 Wetherill Hall, 560 Oval Drive, West Lafayette, Indiana 47907-2084, United States.

Notes
The authors declare no competing financial interest.

ACKNOWLEDGMENTS

■ REFERENCES

(1) *Chlorophylls and Bacteriochlorophylls*; Grimm, B., Porra, R. J., Rüdiger, W., Scheer, H., Eds.; Springer: Dordrecht, NL, 2006; Vol. 25.

(2) *The Purple Phototrophic Bacteria*; Hunter, C. N., Daldal, F., Thurnauer, M. C., Beatty, J. T., Eds.; Springer: Dordrecht, NL, 2009; Vol. 28.

(3) (a) Smith, K. M.; Goff, D. A.; Fajer, J.; Barkigia, K. M. *J. Am. Chem. Soc.* **1982**, *104*, 3747−3749. (b) Barkigia, K. M.; Gottfried, D. S.; Boxer, S. G.; Fajer, J. *J. Am. Chem. Soc.* **1989**, *111*, 6444−6446.

(4) Senge, M. O.; Smith, N. W.; Smith, K. M. *Inorg. Chem.* **1993**, *32*, 1259−1265.

(5) (a) Barkigia, K. M.; Renner, M. W.; Furenlid, L. R.; Medforth, C. J.; Smith, K. M.; Fajer, J. *J. Am. Chem. Soc.* **1993**, *115*, 3627−3635. (b) Shelnutt, J. A.; Song, X.-Z.; Ma, J.-G.; Jentzen, W.; Medforth, C. J. *Chem. Soc. Rev.* **1998**, *27*, 31−41. (c) Senge, M. O. *The Porphyrin Handbook*, Kadish, K. M., Smith, K. M., Guilard, R., Eds.; Academic Press: San Diego, 2000; Vol. 1, 239−347. (d) Senge, M. O.; Renner, M. W.; Kalisch, W. W.; Fajer, J. *Dalton* **2000**, 381−385. (e) Fajer, J. *J. Porphyrins Phthalocyanines* **2000**, *4*, 382−385. (f) Haddad, R. E.; Gazeau, S.; Pécaut, J.; Marchon, J.-C.; Medforth, C. J.; Shelnutt, J. A. *J. Am. Chem. Soc.* **2003**, *125*, 1253−1268. (g) Senge, M. O. *Chem. Commun.* **2006**, 243−256. (h) Senge, M. O.; MacGowan, S. A.; O'Brien, J. M. *Chem. Commun.* **2015**, *51*, 17031−17063.

(6) (a) Kratky, C.; Waditschatka, R.; Angst, C.; Johansen, J. E.; Plaquevent, J. C.; Schreiber, J.; Eschenmoser, A. *Helv. Chim. Acta* **1985**, *68*, 1312−1337. (b) Gudowska-Nowak, E.; Newton, M.; Fajer, J. *J. Phys. Chem.* **1990**, *94*, 5795−5801. (c) Linnanto, J.; Korppi-Tommola, J. *J. Phys. Chem. A* **2004**, *108*, 5872−5882. (d) Zucchelli, G.; Brogioli, D.; Casazza, A. P.; Garlaschi, F. M.; Jennings, R. C. *Biophys. J.* **2007**, *93*, 2240−2254. (e) Bednarczyk, D.; Dym, O.; Prabahar, V.; Peleg, Y.; Pike, D. H.; Noy, D. *Angew. Chem., Int. Ed.* **2016**, *55*, 6901−6905. (f) Wondimagegn, T.; Ghosh, A. *J. Phys. Chem. B* **2000**, *104*, 10858−10862.

(7) (a) MacGowan, S. A.; Senge, M. O. *Chem. Commun.* **2011**, *47*, 11621−11623. (b) Samankumara, L. P.; Wells, S.; Zeller, M.; Acuña, A. M.; Röder, B.; Brückner, C. *Angew. Chem., Int. Ed.* **2012**, *51*, 5757−5760. (c) MacGowan, S. A.; Senge, M. O. *Biochim. Biophys. Acta, Bioenerg.* **2016**, *1857*, 427−442.

(8) Brückner, C. *Acc. Chem. Res.* **2016**, *49*, 1080−1092.

(9) (a) Arnold, L.; Müllen, K. *J. Porphyrins Phthalocyanines* **2011**, *15*, 757−779. (b) Brückner, C.; Akhigbe, J.; Samankumara, L. In *Handbook of Porphyrin Science*; Kadish, K. M., Smith, K. M., Guilard, R., Eds.; World Scientific: River Edge, NY, 2014; Vol. 31, pp 1−276. (c) Costa, L. D.; Costa, J. I.; Tome, A. C. *Molecules* **2016**, *21*, 320.

(10) (a) Ghosh, A. *J. Phys. Chem. B* **1997**, *101*, 3290−3297. (b) Parusel, A. B. J.; Ghosh, A. *J. Phys. Chem. A* **2000**, *104*, 2504−2507. (c) Linnanto, J.; Korppi-Tommola, J. *Phys. Chem. Chem. Phys.* **2006**, *8*, 663−687. (d) Mazzone, G.; Alberto, M. E.; De Simone, B. C.; Marino, T.; Russo, N. *Molecules* **2016**, *21*, 288−299.

(11) Gouterman, M. In *The Porphyrins*; Dolphin, D., Ed.; Academic Press: New York, 1978; Vol. 3, pp 1−165.

(12) Cerussi, A. E.; Berger, A.; Bevilacqua, F.; Shah, N.; Jakubowski, D.; Butler, J.; Holcombe, R. F.; Tromberg, B. J. *Acad. Radiol.* **2001**, *8*, 211−218.

(13) (a) Chen, Y.; Sumlin, A.; Morgan, J.; Gryshuk, A.; Oseroff, A.; Henderson, B. W.; Dougherty, T. J.; Pandey, R. K. *J. Med. Chem.* **2004**, *47*, 4814−4817. (b) Chen, Y.; Li, G.; Pandey, R. K. *Curr. Org. Chem.* **2004**, *8*, 1105−1134. (c) Pandey, R. K.; Zheng, G. In *The Porphyrin Handbook*; Kadish, K. M., Smith, K. M., Guilard, R., Eds.; Academic Press: San Diego, 2000; Vol. 6, pp 157−230. (d) Fukuzumi, S.; Ohkubo, K.; Zheng, X.; Chen, Y.; Pandey, R. K.; Zhan, R.; Kadish, K. M. *J. Phys. Chem. B* **2008**, *112*, 2738−2746. (e) Mroz, P.; Huang, Y.-Y.; Szokalska, A.; Zhiyentayev, T.; Janjua, S.; Nifli, A.-P.; Sherwood, M. E.; Ruzie, C.; Borbas, K. E.; Fan, D.; Krayer, M.; Balasubramanian, T.; Yang, E.; Kee, H. L.; Kirmaier, C.; Diers, J. R.; Bocian, D. F.; Holten, D.; Lindsey, J. S.; Hamblin, M. R. *FASEB J.* **2010**, *24*, 3160−3170.

(f) Huang, Y.-Y.; Mroz, P.; Zhiyentayev, T.; Sharma, S. K.; Balasubramanian, T.; Ruzie, C.; Krayer, M.; Fan, D.; Borbas, K. E.; Yang, E.; Kee, H. L.; Kirmaier, C.; Diers, J. R.; Bocian, D. F.; Holten, D.; Lindsey, J. S.; Hamblin, M. R. *J. Med. Chem.* **2010**, *53*, 4018−4027. (g) Huang, L.; Huang, Y.-Y.; Mroz, P.; Tegos, G. P.; Zhiyentayev, T.; Sharma, S. K.; Lu, Z.; Balasubramanian, T.; Krayer, M.; Ruzie, C.; Yang, E.; Kee, H. L.; Kirmaier, C.; Diers, J. R.; Bocian, D. F.; Holten, D.; Lindsey, J. S.; Hamblin, M. R. *Antimicrob. Agents Chemother.* **2010**, *54*, 3834−3841. (h) Mroz, P.; Huang, Y.-Y.; Janjua, S.; Zhiyentayev, T.; Ruzie, C.; Borbas, K. E.; Fan, D.; Krayer, M.; Balasubramanian, T.; Yang, E. K.; Kee, H. L.; Holten, D.; Lindsey, J. S.; Hamblin, M. R. *Proc. SPIE* **2009**, *7380*, 73802S. (i) O'Connor, A. E.; Gallagher, W. M.; Byrne, A. T. *Photochem. Photobiol.* **2009**, *85*, 1053−1074.

(14) (a) Weissleder, R.; Pittet, M. J. *Nature* **2008**, *452*, 580−589. (b) Brückner, C.; Samankumara, L.; Ogikubo, J. In *Handbook of Porphyrin Science*; Kadish, K. M., Smith, K. M., Guilard, R., Eds.; World Scientific: River Edge, NY, 2012; Vol. 17, pp 1−112. (c) Yang, E.; Diers, J. R.; Huang, Y. Y.; Hamblin, M. R.; Lindsey, J. S.; Bocian, D. F.; Holten, D. *Photochem. Photobiol.* **2013**, *89*, 605−618. (d) Vairaprakash, P.; Yang, E.; Sahin, T.; Taniguchi, M.; Krayer, M.; Diers, J. R.; Wang, A.; Niedzwiedzki, D. M.; Kirmaier, C.; Lindsey, J. S.; Bocian, D. F.; Holten, D. *J. Phys. Chem. B* **2015**, *119*, 4382−4395. (e) Huang, H.; Song, W.; Rieffel, J.; Lovell, J. F. *Front. Phys.* **2015**, *3*, 23.

(15) (a) Goldshaid, L.; Rubinstein, E.; Brandis, A.; Segal, D.; Leshem, N.; Brenner, O.; Kalchenko, V.; Eren, D.; Yecheskel, T.; Salitra, Y.; Salomon, Y.; Scherz, A. *Breast Cancer Res.* **2010**, *12*, R29. (b) Singh, S.; Aggarwal, A.; Thompson, S.; Tome, J. P. C.; Zhu, X.; Samaroo, D.; Vinodu, M.; Gao, R.; Drain, C. M. *Bioconjugate Chem.* **2010**, *21*, 2136−2146. (c) Lovell, J. F.; Jin, C. S.; Huynh, E.; Jin, H.; Kim, C.; Rubinstein, J. L.; Chan, W. C. W.; Cao, W.; Wang, L. V.; Zheng, G. *Nat. Mater.* **2011**, *10*, 324−332. (d) Ethirajan, M.; Chen, Y.; Joshi, P.; Pandey, R. K. *Chem. Soc. Rev.* **2011**, *40*, 340−362.

(16) Takano, K.; Sasaki, S.-i.; Citterio, D.; Tamiaki, H.; Suzuki, K. *Analyst* **2010**, *135*, 2334−2339.

(17) (a) Stromberg, J. R.; Marton, A.; Kee, H. L.; Kirmaier, C.; Diers, J. R.; Muthiah, C.; Taniguchi, M.; Lindsey, J. S.; Bocian, D. F.; Meyer, G. J.; Holten, D. *J. Phys. Chem. C* **2007**, *111*, 15464−15478. (b) Springer, J. W.; Parkes-Loach, P. S.; Reddy, K. R.; Krayer, M.; Jiao, J.; Lee, G. M.; Niedzwiedzki, D. M.; Harris, M. A.; Kirmaier, C.; Bocian, D. F.; Lindsey, J. S.; Holten, D.; Loach, P. A. *J. Am. Chem. Soc.* **2012**, *134*, 4589−4599. (c) Diers, J. R.; Tang, Q.; Hondros, C. J.; Chen, C.-Y.; Holten, D.; Lindsey, J. S.; Bocian, D. F. *J. Phys. Chem. B* **2014**, *118*, 7520−7532.

(18) Krayer, M.; Yang, E.-K.; Diers, J. R.; Bocian, D. F.; Holten, D.; Lindsey, J. S. *New J. Chem.* **2011**, *35*, 587−601. (b) Aravindu, K.; Krayer, M.; Kim, H.-J.; Lindsey, J. S. *New J. Chem.* **2011**, *35*, 1376−1384. (c) Ruzie, C.; Krayer, M.; Balasubramanian, T.; Lindsey, J. S. *J. Org. Chem.* **2008**, *73*, 5806−5820. (d) Fan, D.; Taniguchi, M.; Lindsey, J. S. *J. Org. Chem.* **2007**, *72*, 5350−5357. (e) Kim, H.-J.; Lindsey, J. S. *J. Org. Chem.* **2005**, *70*, 5475−5486.

(19) Senge, M. O.; Wiehe, A.; Ryppa, C. *Adv. Photosynth. Respir.* **2006**, *25*, 27−37.

(20) (a) Whitlock, H. W., Jr.; Hanauer, R.; Oester, M. Y.; Bower, B. K. *J. Am. Chem. Soc.* **1969**, *91*, 7485−7489. (b) Pereira, M. M.; Abreu, A. R.; Goncalves, N. P. F.; Calvete, M. J. F.; Simões, A. V. C.; Monteiro, C. J. P.; Arnaut, L. G.; Eusébio, M. E.; Canotilho, J. *Green Chem.* **2012**, *14*, 1666−1672. (c) Pereira, M. M.; Monteiro, C. J. P.; Simoes, A. V. C.; Pinto, S. M. A.; Abreu, A. R.; Sa, G. F. F.; Silva, E. F. F.; Rocha, L. B.; Dabrowski, J. M.; Formosinho, S. J.; Simoes, S.; Arnaut, L. G. *Tetrahedron* **2010**, *66*, 9545−9551. (d) Silva, E. F. F.; Serpa, C.; Dabrowski, J. M.; Monteiro, C. J. P.; Formosinho, S. J.; Stochel, G.; Urbanska, K.; Simoes, S.; Pereira, M. M.; Arnaut, L. G. *Chem. - Eur. J.* **2010**, *16*, 9273−9286.

(21) (a) Moura, N. M. M.; Giuntini, F.; Faustino, M. A. F.; Neves, M. G. P. M. S.; Tome, A. C.; Silva, A. M. S.; Rakib, E. M.; Hannioui, A.; Abouricha, S.; Roder, B.; Cavaleiro, J. A. S. *ARKIVOC* **2010**, 24−33. (b) Tome, A. C.; Neves, M. G. P. M. S.; Cavaleiro, J. A. S. *J. Porphyrins Phthalocyanines* **2009**, *13*, 408−414. (c) Silva, A. M. G.; Cavaleiro, J. A. S. *Prog. Heterocycl. Chem.* **2008**, *19*, 44−69. (d) Silva, A. M. G.; Tome,

A. C.; Neves, M. G. P. M. S.; Cavaleiro, J. A. S.; Perrone, D.; Dondoni, A. *Synlett* **2005**, 857−859. (e) Cavaleiro, J. A. S.; Neves, M. G. P. M. S.; Tome, A. C. *ARKIVOC* **2003**, 107−130.

(22) (a) Starnes, S. D.; Rudkevich, D. M.; Rebek, J., Jr. *J. Am. Chem. Soc.* **2001**, *123*, 4659−4669. (b) Sutton, J. M.; Clarke, O. J.; Fernandez, N.; Boyle, R. W. *Bioconjugate Chem.* **2002**, *13*, 249−263.

(23) Bruhn, T.; Brückner, C. *J. Org. Chem.* **2015**, *80*, 4861−4868.

(24) Samankumara, L. P.; Zeller, M.; Krause, J. A.; Brückner, C. *Org. Biomol. Chem.* **2010**, *8*, 1951−1965.

(25) Ke, X.-S.; Chang, Y.; Chen, J.-Z.; Tian, J.; Mack, J.; Cheng, X.; Shen, Z.; Zhang, J.-L. *J. Am. Chem. Soc.* **2014**, *136*, 9598−9607.

(26) (a) Cetin, A.; Ziegler, C. J. *Dalton Trans.* **2005**, 25−26. (b) Liang, L.; Lv, H.; Yu, Y.; Wang, P.; Zhang, J.-L. *Dalton Trans.* **2012**, *41*, 1457−1460. (c) Tang, J.; Chen, J.-J.; Jing, J.; Chen, J.-Z.; Lv, H.; Yu, Y.; Xu, P.; Zhang, J.-L. *Chem. Sci.* **2014**, *5*, 558−566. (d) Ke, X. S.; Yang, B. Y.; Cheng, X.; Chan, S. L. F.; Zhang, J. L. *Chem. - Eur. J.* **2014**, *20*, 4324−4333. (e) Ke, X.-S.; Tang, J.; Chen, J.-J.; Zhou, Z.-Y.; Zhang, J.-L. *ChemPlusChem* **2015**, *80*, 237−252.

(27) (a) Brückner, C.; Rettig, S. J.; Dolphin, D. *J. Org. Chem.* **1998**, *63*, 2094−2098. (b) McCarthy, J. R.; Jenkins, H. A.; Brückner, C. *Org. Lett.* **2003**, *5*, 19−22. (c) Brückner, C.; Götz, D. C. G.; Fox, S. P.; Ryppa, C.; McCarthy, J. R.; Bruhn, T.; Akhigbe, J.; Banerjee, S.; Daddario, P.; Daniell, H. W.; Zeller, M.; Boyle, R. W.; Bringmann, G. *J. Am. Chem. Soc.* **2011**, *133*, 8740−8752.

(28) Abuteen, A.; Zanganeh, S.; Akhigbe, J.; Samankumara, L. P.; Aguirre, A.; Biswal, N.; Braune, M.; Vollertsen, A.; Röder, B.; Brückner, C.; Zhu, Q. *Phys. Chem. Chem. Phys.* **2013**, *15*, 18502−18509.

(29) The spectroscopic data for all novel compounds, together with a reproduction of their spectra, are presented in the SI.

(30) RMSD values listed are the root-mean-square values of the deviation from planarity for the bacteriochlorin chromophore, calculated as $\text{RMSD} = \sqrt{\frac{1}{20}(x_1{}^2 + x_2{}^2 + ... + x_{20}{}^2)}$ where x is the out-of-plane deviation for each of the 20 atoms of the $C_{16}N_4$ macrocycle (i.e., excluding all pyrroline and morpholine b- and O-atoms).

(31) Fässler, A.; Pfaltz, A.; Müller, P. M.; Farooq, S.; Kratky, C.; Kräutler, B.; Eschenmoser, A. *Helv. Chim. Acta* **1982**, *65*, 812−827.

(32) Molecular graphics images produced using UCSF Chimera (V. 1.5.3), University of California, San Francisco, supported by NIH P41 RR001081.

(33) Daniell, H. W.; Brückner, C. *Angew. Chem., Int. Ed.* **2004**, *43*, 1688−1691.

(34) Hyland, M. A.; Hewage, N.; Panther, K.; Nimthong Roldan, A.; Zeller, M.; Samaraweera, M.; Gascon, J. A.; Brückner, C. *J. Org. Chem.* **2016**, *81*, 3603−3618.

(35) Ryeng, H.; Ghosh, A. *J. Am. Chem. Soc.* **2002**, *124*, 8099−8103.

(36) Fox, S.; Boyle, R. W. *Tetrahedron* **2006**, *62*, 10039−10054.

(37) (a) Ridley, J.; Zerner, M. *Theor. Chim. Acta* **1973**, *32*, 111−134. (b) Ridley, J. E.; Zerner, M. C. *Theor. Chim. Acta* **1976**, *42*, 223−236. (c) Zerner, M. C.; Loew, G. H.; Kirchner, R. F.; Mueller-Westerhoff, U. T. *J. Am. Chem. Soc.* **1980**, *102*, 589−599.

(38) (a) Barone, V.; Cossi, M. *J. Phys. Chem. A* **1998**, *102*, 1995−2001. (b) Cossi, M.; Rega, N.; Scalmani, G.; Barone, V. *J. Comput. Chem.* **2003**, *24*, 669−681.

(39) Frisch, M. J.; Trucks, G. W.; Schlegel, H. B.; Scuseria, G. E.; Robb, M. A.; Cheeseman, J. R.; Scalmani, G.; Barone, V.; Mennucci, B.; Petersson, G. A.; Nakatsuji, H.; Caricato, M.; Li, X.; Hratchian, H. P.; Izmaylov, A. F.; Bloino, J.; Zheng, G.; Sonnenberg, J. L.; Hada, M.; Ehara, M.; Toyota, K.; Fukuda, R.; Hasegawa, J.; Ishida, M.; Nakajima, T.; Honda, Y.; Kitao, O.; Nakai, H.; Vreven, T.; Montgomery, J. A., Jr.; Peralta, J. E.; Ogliaro, F.; Bearpark, M.; Heyd, J. J.; Brothers, E.; Kudin, K. N.; Staroverov, V. N.; Kobayashi, R.; Normand, J.; Raghavachari, K.; Rendell, A.; Burant, J. C.; Iyengar, S. S.; Tomasi, J.; Cossi, M.; Rega, N.; Millam, J. M.; Klene, M.; Knox, J. E.; Cross, J. B.; Bakken, V.; Adamo, C.; Jaramillo, J.; Gomperts, R.; Stratmann, R. E.; Yazyev, O.; Austin, A. J.; Cammi, R.; Pomelli, C.; Ochterski, J. W.; Martin, R. L.; Morokuma, K.; Zakrzewski, V. G.; Voth, G. A.; Salvador, P.; Dannenberg, J. J.; Dapprich, S.; Daniels, A. D.; Farkas, O.; Foresman, J. B.; Ortiz, J. V.; Cioslowski, J.; Fox, D. J. *Gaussian 09*, revision D.01; Gaussian, Inc.: Wallingford, CT, 2009.

(40) MacGowan, S. A.; Senge, M. O. *Inorg. Chem.* **2013**, *52*, 1228−1237.

(41) Parusel, A. B.; Wondimagegn, T.; Ghosh, A. *J. Am. Chem. Soc.* **2000**, *122*, 6371−6374.

(42) Luciano, M.; Tardie, W.; Zeller, M.; Brückner, C. *Chem. Commun.* **2016**, *52*, 10133−10136.

(43) Jentzen, W.; Simpson, M. C.; Hobbs, J. D.; Song, X.; Ema, T.; Nelson, N. Y.; Medforth, C. J.; Smith, K. M.; Veyrat, M.; Mazzanti, M.; Ramasseul, R.; Marchon, J. C.; Takeuchi, T.; Goddard, W. A.; Shelnutt, J. A. *J. Am. Chem. Soc.* **1995**, *117*, 11085−11097.

(44) Jiang, Y. *Mater. Sci. Eng., C* **2014**, *45*, 682−689.

(45) (a) Becke, A. D. *J. Chem. Phys.* **1993**, *98*, 5648−5652. (b) Stephens, P.; Devlin, F.; Chabalowski, C.; Frisch, M. J. *J. Phys. Chem.* **1994**, *98*, 11623−11627.